Solubilization Behavior of *n*-Octane and *n*-Octanol in Polyoxyethylated Nonionic Micelles

Yoshihiro Saito[a,*], **Masahiko Abe**[b] and **Takatoshi Sato**[a]

[a]Nihon University, College of Pharmacy, 7-1, Narashinodai, 7-Chome, Funabashi-shi, Chiba, Japan and [b]Faculty of Science and Technology, Science University of Tokyo, 2641, Yamazaki, Noda-shi, Chiba, Japan

The solubilization of *n*-octane and *n*-octanol in nonionic micelles was investigated by means of various techniques including solubilization, fluorescence and dynamic light-scattering measurements. With respect to the effect of oxyethylene chainlength of the surfactants, different solubilization behavior was observed between *n*-octane and *n*-octanol, *i.e.*, the solubilization of *n*-octane decreases with an increase in oxyethylene chainlength, while that of *n*-octanol increases. This solubilization behavior is explained from the standpoint of the volume of hydrophobic and hydrophilic regions in a micelle.

KEY WORDS: Micellar structure, micelle characteristics, microscopic polarity, nonionic surfactant, solubilization mechanism.

The solubility of many organic compounds that have limited solubility in water can be increased considerably by the addition of a nonionic surfactant. Knowledge of the micellar structure of nonionic surfactants is of fundamental importance in understanding the solubilizing process. Therefore, the effects of micellar properties on the solubilization mechanism have been investigated by various authors (1,2). Recently, several studies on the solubilization mechanism of linear additive molecules, such as *n*-alkanes and *n*-alkanols, have been reported, including a series of studies on sodium dodecyl sulfate (3–5), one study on thermodynamics (6) and solubilization by a mixed surfactant system (7). Linear additive molecules are convenient in the discussion of the solubilization mechanism because they typically cause less disturbance to the micellar structure than other bulkier solubilizates (8).

Here we report mainly the effects of the volume of hydrophobic and hydrophilic regions in a micelle on the solubilization mechanism of *n*-octane and *n*-octanol by nonionic surfactants.

EXPERIMENTAL PROCEDURES

Materials. The nonionic surfactants polyoxyethylene lauryl ethers ($C_{12}E_n$, n = 9, 12 or 19, where n is the average number of ethylene oxide groups) were obtained from Kao Co., Ltd. (Tokyo, Japan) and were used as received. *n*-Octane and *n*-octanol of the purest grade were obtained from Wako Pure Chemical Industries Ltd. (Tokyo, Japan) and were rated as more than 98.5% pure. The fluorescence probe, *i.e.*, pyrene, was purchased from Wako Pure Chemical Industries Ltd. and chromatographed on silica gel with *n*-hexane as an eluent (9).

Solubilization measurements. The following procedure was the design for the limits of solubilization: Into several 50-mL glass-stoppered vials, 20 mL aliquots of solution of various $C_{12}E_n$ concentrations were added; then varying amounts of *n*-octane or *n*-octanol were combined with these solutions by microsyringe. The mixtures were shaken while being stirred (24 h for *n*-octanol, 48 h for *n*-octane), at 25°C, to attain equilibrium. These times were found to be sufficient for equilibrium to be attained. After equilibrium had been established in experiments with *n*-octanol, the turbidity of the solutions was measured with a turbidimeter (Tokyo Koden, Tokyo, Japan; Model ANA-14A). The turbidity concentration obtained was extrapolated to zero to obtain the amount of solubilization (3–5). However, this method could not be used for *n*-octane because it is very insoluble in water, and *n*-octane droplets float on the upper part of $C_{12}E_n$ aqueous solutions. Therefore, the limiting point of solubilization of *n*-octane was determined by visual inspection for faint turbidity and/or a trace of oil droplets under white fluorescent light.

Viscosity measurements. An Ubbelohde viscometer was used to measure the viscosity of the $C_{12}E_n$ solutions.

Fluorescence measurements. Fluorescence characteristics of pyrene were determined with a Japan Spectroscopic (Tokyo, Japan) fluorescence spectrophotometer, Model FP-770. Emission spectra of the pyrene were obtained by exciting the pyrene at 338.0 nm. The concentration of pyrene for fluorescence measurements was 2.0×10^{-6} mol/L.

Dynamic light-scattering measurements. The dynamic light-scattering measurements were performed with a 4700-type submicron particle analyzer (Malvern Co., Worchestershire, United Kingdom), with a multibit (8 × N) Malvern correlator with delayed channels. The correlator was interfaced to a PC-AT IBM computer, allowing continuous control of the base line. The light source was an argon ion laser (Coherent Co., Innova 90; Palo Alto, CA), used at a wavelength of 488 nm and a power source of 5 W.

Study of the $C_{12}E_n$ micellar shape was undertaken by examining the relation between the reciprocal of the diffusion coefficient and the scattering vector (10). Solutions were purified by ultrafiltration through 0.22-μm Millipore filters (Nihon Millipore Kogga, Yonezawa, Japan). The above experiments were measured at 25°C.

RESULTS AND DISCUSSION

Characteristics of $C_{12}E_n$ micelles. The $C_{12}E_n$ micelles used in the present investigation are all spherical (11), and the dependence of micellar molecular weight (M_m) on the oxyethylene chainlength (m) for a series of $C_{12}E_n$ is given by relation (12):

$$M_m = A_n M = (1025/m - 5.1)M \quad [1]$$

where A_n is the aggregation number and M is the molecular weight of $C_{12}E_n$. Also, the micellar volume, including hydration (V_h), can be calculated from the intrinsic viscosity ([η]) (13):

$$V_h = [\eta]M_m/2.5N \quad [2]$$

where N is Avogadro's number. In addition, the volume of the hydrocarbon core (V_c) and the volume of the

*To whom correspondence should be addressed.

TABLE 1

Characteristics of Spherical Micelles of $C_{12}E_n$ in Aqueous Solution[a]

	$M_m \times 10^3$	A_n	$[\eta]$ (cm^3/g)	$V_h \times 10^4$ (Å^3)	$V_C \times 10^4$ (Å^3)	$V_{OE} \times 10^4$ (Å^3)
$C_{12}E_9$	63.3	109	6.1	25.7	3.81	21.9
$C_{12}E_{12}$	57.3	80	6.9	26.3	2.80	23.5
$C_{12}E_{19}$	49.9	54	8.1	26.9	1.89	25.0

[a]Abbreviations: $C_{12}E_n$, n = 9, 12 or 19–the nonionic surfactants polyoxyethylene lauryl ethers; M_m, micellar molecular weight; A_n, aggregation number; $[\eta]$, intrinsic viscosity; V_h, micellar volume including hydration; V_c, volume of the hydrocarbon core; V_{OE}, volume of the palisade layer of ethylene oxide units.

palisade layer of ethylene oxide units (V_{OE}), that is, the hydrophilic region in $C_{12}E_n$ micelles, were estimated from the following equations (Refs. 14–16):

$$V_c = A_n V = 10^{24} A_n M_c / dN \quad [3]$$

$$V_{OE} = V_h - V_c \quad [4]$$

where V is the volume of alkyl chain in a single $C_{12}E_n$ molecule, M_c is its molecular weight and d is the density (0.802 g cm^{-3}) of the corresponding liquid *n*-alkane at 25°C.

Table 1 shows the characteristics of $C_{12}E_n$ micelles. The micellar molecular weight and the aggregation number decreased while the micellar volume increased with an increase in the oxyethylene chainlength. Trends are those expected for nonionic surfactants (17,18). Also, the volume of the hydrocarbon core decreased while the volume of the hydrophilic region increased with an increase in oxyethylene chainlength of $C_{12}E_n$. The tendency of an increasing volume of the hydrophilic region with an increase in oxyethylene chainlength met our expectation and was easily interpreted. However, it is unclear why the V_c decreases with an increase in the oxyethylene chainlength in spite of the fact the same alkyl chainlength is maintained. Equation 3 indicates that the V_c may be closely correlated with the aggregation number. Schott (19,20) has also reported similar results for the V_c of $C_{12}E_{16}$ and $C_{12}E_{28}$ micelles. Assuming the micelles to be spherical, with a core consisting of a hydrocarbon droplet of the same density as the bulk density of the hydrocarbon moiety of the surfactant, the V_c was calculated in either case. However, the aggregation numbers used in the calculation by Schott were obtained by means of the dye solubilization method. Those in this study were obtained by the light-scattering method. Though dye solubilization is not an absolute method for determining aggregation number, the numbers obtained by dye solubilization and light-scattering methods correlate well for nonionic surfactants.

Distribution coefficient and standard free energy change. The solubilities of *n*-octane and *n*-octanol increased linearly with an increase in $C_{12}E_n$ concentration; so, the distribution coefficient (K) of the solubilizates between the water and micellar phases was calculated by the equation of Blokhus *et al.* (21):

$$K = X_{sol}^{mic}/X_{sol}^{aq} = [n_{sol}^{mic}/(n_{sol}^{mic} + n_{sur}^{mic})]/[n_{sol}^{aq}/(n_{sol}^{aq} + n_{sur}^{aq} + nH_2O)] \quad [5]$$

where X_{sol}^{mic} and X_{sol}^{aq} are the mole fractions of *n*-octane or *n*-octanol in the micellar and aqueous phases, n_{sol}^{mic} and n_{sol}^{aq} are the number of moles in each phase, and nH_2O is the number of moles of water. The subscript "sur" represents "surfactant." Equation 5 can be rearranged to read:

$$m_{sol}^{lim} = KM_{H_2O} m_{sol}^{aq} (m_{sur}^{tot} - m_{sur}^{CMC})/(1 - KM_{H_2O} m_{sol}^{aq}) + m_{sol}^{aq} \quad [6]$$

where m_{sol}^{lim} is the limit of solubilization of *n*-octane or *n*-octanol, M_{H_2O} is the molar mass of water, m_{sur}^{tot} is the total content of surfactant, m_{sur}^{CMC} is the surfactant content at the critical micelle concentration (CMC) (from Ref. 22) and m_{sol}^{aq} is the solubility of *n*-octane or *n*-octanol in water. The limit of solubilization of *n*-octane or *n*-octanol *vs.* the micellar surfactant content, *i.e.*, *vs.* $(m_{sur}^{tot} - m_{sur}^{CMC})$, indicated a straight line, with an intercept equal to the solubility in water as shown in Figure 1. So, the distribution coefficient was calculated from the slope. Furthermore, the standard free energy change (ΔG_S^0) of solubilization, when one mole of solubilizate transfers from solution to micelle is given by:

$$\Delta G_S^0 = -RT\ln(K) \quad [7]$$

where T is absolute temperature and R is the gas constant.

These parameters are shown in Table 2. For the solubilization of *n*-octane, K values decreased while ΔG_S^0 increased as the oxyethylene chainlength of $C_{12}E_n$ was

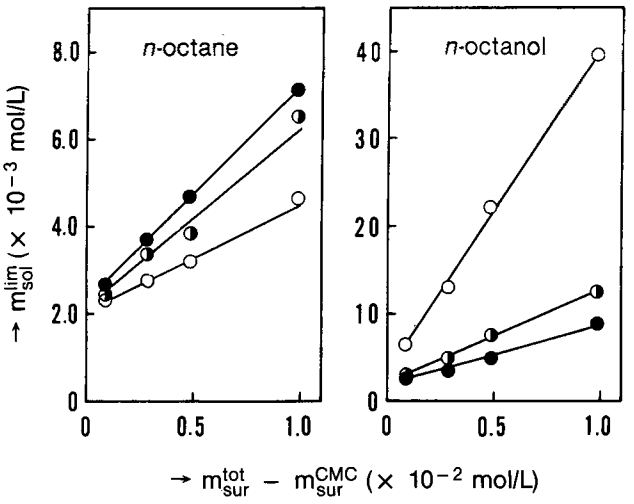

FIG. 1. Total solubilities of *n*-octane and *n*-octanol in $C_{12}E_n$ aqueous solutions: ●, $C_{12}E_9$; ◑, $C_{12}E_{12}$; ○, $C_{12}E_{19}$.

TABLE 2

Distribution Coefficients (K) and Standard Free Energy Changes (ΔG_s^0) of *n*-Octane and *n*-Octanol[a]

	n-Octane		*n*-Octanol	
	$K \times 10^3$	ΔG_s^0 (kcal/mol)	$K \times 10^3$	ΔG_s^0 (kcal/mol)
$C_{12}E_9$	10.1	−5.46	7.04	−5.24
$C_{12}E_{12}$	8.66	−5.37	9.72	−5.43
$C_{12}E_{19}$	6.06	−5.16	15.6	−5.71

[a]See Table 1 for abbreviations.

increased. On the other hand, the solubilization of *n*-octanol showed the reverse tendency, that is, the solubilization of *n*-octanol increased with an increase in oxyethylene chainlength.

These results indicate a distinction between the solubilization mechanism of *n*-octane and *n*-octanol by $C_{12}E_n$. Similar results have also been reported for the solubilization of *n*-hexane and *n*-hexanol by polyethylene glycol *n*-nonylphenyl ethers (23). Commonly, comparisons of micellar aggregation number and micellar size of surfactants have been discussed to explain solubilization (24,25). However, the solubilization mechanisms of *n*-octane and *n*-octanol in this study cannot be explained by these parameters. Also, the spatial effects of hydrophobic and hydrophilic regions in the micelle on the solubilization mechanism have been presumed (7,26). However, no detailed study has yet been reported. Accordingly, we next examined the relationship between V_{OE}/V_C ratio and ΔG_S^0 on the basis of the data shown in Tables 1 and 2. These results are depicted in Figure 2.

For *n*-octane, ΔG_S^0 increased significantly with an increase in the V_{OE}/V_C ratio. This indicates that *n*-octane became more insoluble with an increase in V_{OE} per micelle. On the other hand, ΔG_S^0 of *n*-octanol decreased with an increase in the V_{OE}/V_C ratio. This means that the increase of V_{OE} per individual micelle acts advantageously on the solubilization of *n*-octanol.

Microscopic polarity and site of solubilization. The ratio of intensity of the first peak to the third peak (I_1/I_3) of pyrene emission is a sensitive monitor of the pyrene environment. The parameter I_1/I_3 is also proportional to microscopic polarity (10,27). This unique photophysical feature has been utilized to determine the micropolarity of the surrounding hydrophilic region in the micelle because pyrene is known to reside in the palisade layer of ethylene oxide units (28). Measurements of the I_1/I_3 ratio of pyrene in $C_{12}E_n$ micelles were carried out in the presence of the solubilizates.

As an example, the results for $C_{12}E_{19}$ are shown in Figure 3. The abscissa used in these plots is moles of solubilizates per mole of surfactants ($[m_{sol}/m_{sur}]$). Similar results were also obtained for the other $C_{12}E_n$. The I_1/I_3 ratios of pyrene in the presence of *n*-octanol were greatly influenced by $[m_{sol}/m_{sur}]$ and were significantly lower with increasing concentrations of *n*-octanol. Lower I_1/I_3 ratios of *n*-octanol mean decreases in polarity in the surrounding hydrophilic region. This occurs because *n*-octanol solubilized in the hydrophilic region screens the water penetration within the micelle (9). On the other hand, for *n*-octane, the I_1/I_3 ratios were little affected by the addition of *n*-octane. Also, the I_1/I_3 ratio can be utilized to determine the site of solubilizate within the micelle, as reported by Malliaris (8). The I_1/I_3 ratio of pyrene in the micelle is not affected by the addition of *n*-alkanes but is greatly affected by the addition of *n*-alkanols. This demonstrates that alkanes solubilize in the micellar interior, and alkanols solubilize in the hydrophilic region, as does pyrene. From the results shown in Figure 3, it is thought that *n*-octane in $C_{12}E_n$ micelles is located in the micellar core, and *n*-octanol is in the palisade layer of ethylene oxide units of nonionic surfactants.

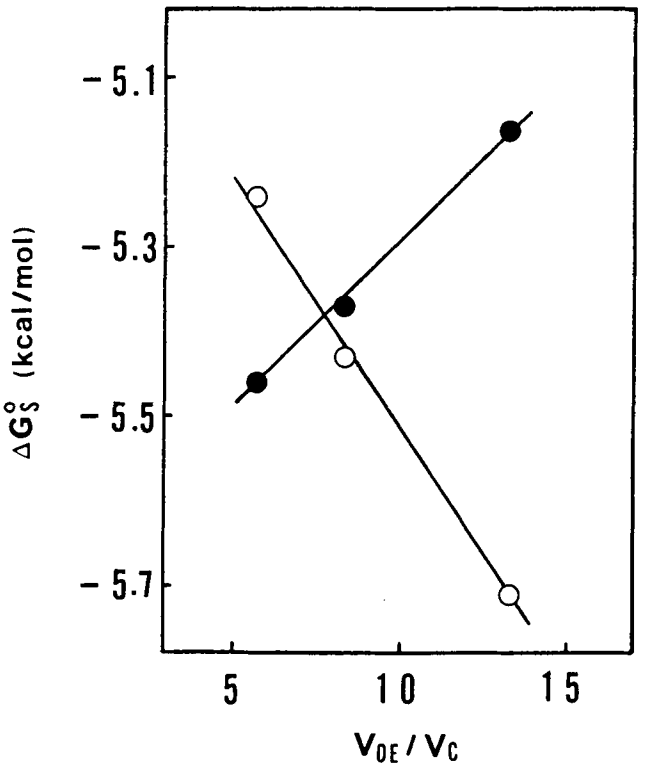

FIG. 2. Relationship between the volume of the palisade layer of ethylene oxide units/volume of the hydrocarbon core V_{OE}/V_c ratio and ΔG_S^0 of solubilization of *n*-octane and *n*-octanol: ●, *n*-octane; ○, *n*-octanol.

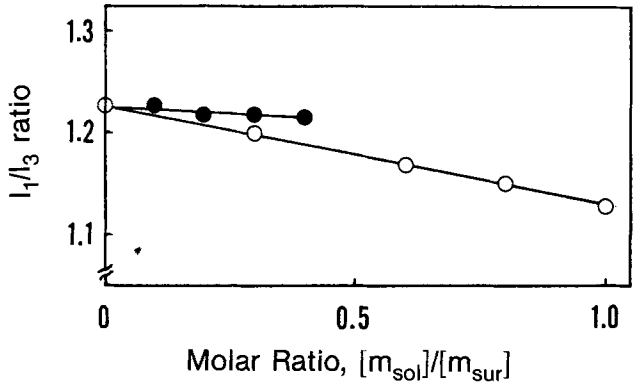

FIG. 3. Plots of I_1/I_3 ratio of pyrene *vs.* $[m_{sol}/m_{sur}]$ in $C_{12}E_{19}$ aqueous solution: ●, *n*-octane; ○, *n*-octanol, sol, solubilizates, sur, surfactant.

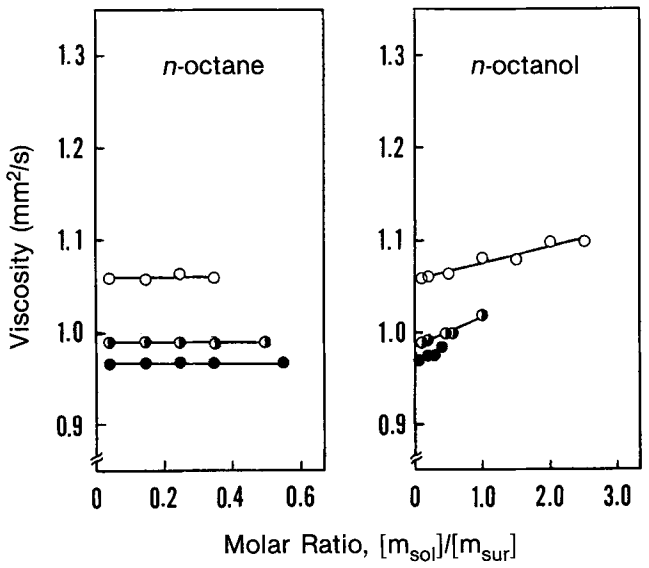

FIG. 4. Kinematic viscosities of $C_{12}E_n$ solutions as a function of $[m_{sol}/m_{sur}]$: ●, $C_{12}E_9$; ◑, $C_{12}E_{12}$; ○, $C_{12}E_{19}$. Abbreviations as in Figure 3.

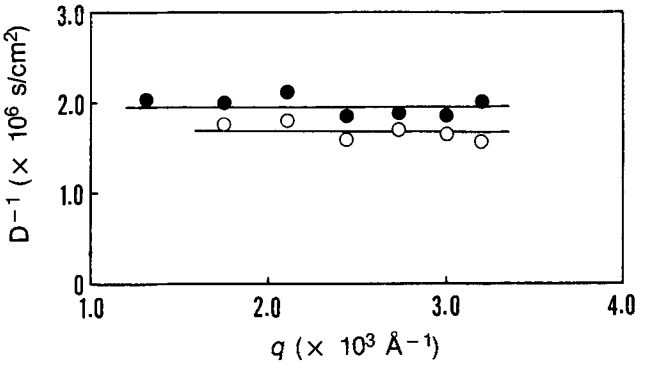

FIG. 5. Plots of D^{-1} *vs.* q for $C_{12}E_{19}$ micelle in the presence of *n*-octanol: ○, $[m_{sol}/m_{sur}] = 1.0$; ●, $[m_{sol}/m_{sur}] = 2.5$. Abbreviations as in Figure 3.

Considering the results shown in Figures 2 and 3, it could be surmised that the solubility of *n*-octane increases with an increase in the volume of the core region because *n*-octane is located within the micellar core. On the other hand, the site of *n*-octanol is within the surrounding hydrophilic region, and so a large hydrophilic region is thought to be advantageous for the solubilization of *n*-octanol. Thus, the solubilization mechanisms of *n*-octane and *n*-octanol are correlated with not only the micellar aggregation number and the micellar size but also with the volume of the solubilized site.

Micelle characteristics after solubilization. Micelle characteristics after solubilization of *n*-octane and *n*-octanol were investigated by kinematic viscosity measurements.

Figure 4 shows changes of the kinematic viscosity of $C_{12}E_n$ micelles after solubilization as a function of $[m_{sol}/m_{sur}]$. The kinematic viscosity of all $C_{12}E_n$ in the presence of *n*-octane was altered little by $[m_{sol}/m_{sur}]$. This means that the shape and size of $C_{12}E_n$ micelles do not change with the addition of *n*-octane (7). However, for *n*-octanol, the kinematic viscosity demonstrated large increases with an increase in *n*-octanol concentration. This result is most likely due to an increase in aggregate size and/or stronger intermicellar interactions (29). Similarly, Kandori and co-workers (26) reported that phenol solubilized into the palisade layer making up the hydrophilic region leads to a greater increase in the viscosity of cationic micelles than the addition of benzene solubilized in the core region. From the viscosity data alone, the reason for a larger kinematic viscosity in the case of *n*-octanol cannot be proven to be either an increase in micellar size or an increase in interparticle interaction. Further investigation of $C_{12}E_n$ micelles characteristics in the presence of *n*-octanol was carried out by examining the relation between the reciprocal of the diffusion coefficient (D^{-1}) and the scattering vector (q) by means of the dynamic light-scattering technique. The scattering vector can be given by (10,30):

$$q = (4\pi n/\lambda)\sin(\theta/2) \quad [8]$$

where n is the refractive index of the solvent, λ is the wavelength of light and θ the scattering angle.

As an example, the results for $C_{12}E_{19}$ are shown in Figure 5. D^{-1} for $[m_{sol}]/[m_{sur}] = 1.0$ and 2.5 did not depend on q. Similar results were also obtained for the other $C_{12}E_n$. D^{-1} for a spherical structure without interparticle interaction does not depend on q, while those values for spherical structures with interparticle interactions and for nonspherical particles depend on q (10,30). Consequently, for *n*-octanol, a large kinematic viscosity is not due to interparticle interaction. Thus, it can be surmised that an increase in micellar size, maintaining spherical shape, occurs as the solubility of *n*-octanol increases.

In conclusion, the solubilization mechanisms of *n*-octane and *n*-octanol by $C_{12}E_n$ micelles appear to be governed mainly by the volume of the hydrophobic and hydrophilic regions in the micelle rather than by micellar size or aggregation number.

REFERENCES

1. Klevens, H.B., *Chem. Rev. 47*:1 (1950).
2. Nakagawa, T., in *Nonionic Surfactants*, edited by M.J. Schick, Marcel Dekker, New York, 1967, pp. 558.
3. Ogino, K., M. Abe and N. Takesita, *Bull. Chem. Soc. Jpn. 49*:3679 (1976).
4. Ogino, K., M. Abe and N. Takesita, *Ibid. 51*:1880 (1978).
5. Abe, M., and K. Ogino, *J. Jpn. Oil Chem. Soc. 31*:569 (1982).
6. Hayase, K., S. Hayano and H. Tsubota, *J. Colloid Interface Sci. 101*:336 (1984).
7. Zhao, G., and L. Xue-gang, *Ibid. 144*:185 (1991).
8. Malliaris, A., *Adv. Colloid Interface Sci. 27*:153 (1987).
9. Abe, M., Y. Tokuoka, H. Uchiyama and K. Ogino, *J. Jpn. Oil Chem. Soc. 39*:565 (1990).
10. Ogino, K., M. Nakamae and M. Abe, *J. Phys. Chem. 93*:3704 (1989).
11. Schick, M.J., S.M. Atlas and F.R. Eirich, *Ibid. 66*:1326 (1962).
12. Becher, P., *J. Colloid Sci. 16*:49 (1961).
13. Saito, Y., and T. Sato, *J. Phys. Chem. 89*:2110 (1985).
14. Schott, H., *J. Pharm. Sci. 60*:1594 (1971).
15. Zografi, G., and S.H. Yalkowsky, *Ibid. 61*:651 (1972).
16. Birdi, K.S., *Prog. Colloid & Polym. Sci. 70*:23 (1985).
17. EL Eini, D.I.D., B.W. Barry and C.T. Rhodes, *J. Colloid Interface Sci. 54*:348 (1976).
18. Birdi, K.S., *Colloid & Polym. Sci. 252*:551 (1974).
19. Schott, H., *J. Phys. Chem. 70*:2966 (1966).

20. Schott, H., *Ibid. 71:*3611 (1967).
21. Blokhus, A.M., H. Hoiland and S. Backlund, *J. Colloid Interface Sci. 114:*9 (1986).
22. Becher, P., *J. Colloid Sci. 17:*325 (1962).
23. Tuji, S., *Nyuuka kayouka no gijyutu*, Kougakutosyo, Japan, 1976, p. 144.
24. Barry, B.W., and D.I.D. EL Eini, *J. Pharm. Pharmacol. 28:*210 (1976).
25. Arnarson, T., and P.H. Elworthy, *Ibid. 33:*141 (1981).
26. Kandori, K., R.J. McGreevy and R.S. Schechter, *J. Phys. Chem. 93:*1506 (1989).
27. Turro, N.J., and P.-L. Kuo, *Ibid. 90:*4205 (1986).
28. Turro, N.J., and P.-L. Kuo, *Langmuir. 2:*438 (1986).
29. Kandori, K., P.J. McGrrvy and R.S. Schechter, *J. Colloid Interface Sci. 132:*395 (1989).
30. Rushforth, D.S., M. Sanchez-Rubio, L.M. Santos-Vidals, K.R. Wormuth, E.W. Kaler, R. Cuevas and J.E. Puig, *J. Phys. Chem. 90:*6668 (1986).

[Received June 23, 1992; accepted March 29, 1993]